Analytical-Numerical Hybrid Method to Determine the Stress Field in Front of the Crack in 3D Elastic-Plastic Structural Element

Andrzej Neimitz[1, a], Marcin Graba[1,b]

[1] Kielce University of Technology, Faculty of Mechatronics and Machine Design, Chair of Fundamentals of Machine Design, Aleja 1000-lecia PP 7, PL - 25 314 Kielce, POLAND

[a]neimitz@tu.kielce.pl, [b]mgraba@tu.kielce.pl

Keywords: fracture, stress distribution, stress field, *Q*-stress, HRR, T_z parameter.

Abstract. Two-term O'Dowd-Shih stress formula to assess the stress field in front of the crack is extended in order to include the influence of the third dimension in the element thickness direction. As a measure of the out-of-plane constraint, the T_z parameter introduced by Guo Wanlin, has been adopted. It is assumed that both the HRR term and the Q^* parameter are functions of T_z. The T_z function is computed numerically. The numerical results are approximated by analytical formulas. The comparison between proposed formulas and full 3D numerical analysis will be presented.

Introduction – theoretical backgrounds for the 2D and 3D fracture mechanics

In 1968 J.W. Hutchinson [1] published the fundamental work, which characterized the stress fields in front of a crack for non-linear Ramberg-Osgood (R-O) material:

$$\sigma_{ij} = \sigma_0 \left(\frac{J}{\alpha \sigma_0 \varepsilon_0 I_n r} \right)^{\frac{1}{1+n}} \tilde{\sigma}_{ij}(\theta, n) \tag{1}$$

where r and θ are polar coordinates of the coordinate system located at the crack tip, σ_{ij} are the components of the stress tensor, J is the J-integral, n is R-O exponent, α is R-O constant, σ_o is yield stress, ε_0 is strain related to σ_o through $\varepsilon_o = \sigma_o/E$. Functions $\tilde{\sigma}_{ij}(n,\theta)$, $I_n(n)$ must be found by solving the fourth order non-linear homogenous differential equation, independently for plane stress and plane strain [1,2]. Equation (1) is usually called the "HRR solution".

In 1993 O'Dowd and Shih [3,4], proposed simplified solution for the stress field which provided more exact results for plane strain and low constraint elements than the HRR formula

$$\sigma_{ij} = \left(\sigma_{ij}\right)_{HRR} + Q\sigma_0 \hat{\sigma}_{ij}(\theta). \tag{2}$$

To avoid the ambiguity during the calculation of the Q-stress, O'Dowd and Shih suggested, that the Q-stress may be evaluated at the distance $r=2J/\sigma_0$ from the crack tip at $\theta=0$. The Q-stress is computed from the following relationship:

$$Q = \frac{(\sigma_{\theta\theta})_{FEM} - (\sigma_{\theta\theta})_{HRR}}{\sigma_0} \quad \text{for } \theta=0 \text{ and } \frac{r\sigma_0}{J} = 2 \tag{3}$$

where $(\sigma_{\theta\theta})_{FEM}$ is the stress value calculated using FEM (Finite Element Method) and $(\sigma_{\theta\theta})_{HRR}$ is stress value evaluated form HRR solution, this term can be replaced by stresses computed for the small scale yielding model. The Q- parameter is a measure of the in-plane-constraint.

Guo extended the HRR analysis in a series of papers [5-7] to the three-dimensional (3D) case. In fact, he showed that the HRR singularity can be obtained for plane strain and plane stress only and in the 3D case the simplified, approximate formula in the form of Eq. (1) was proposed:

$$\sigma_{ij} = \sigma_0 \left(\frac{J^{far}}{\alpha \sigma_0 \varepsilon_0 I(T_z, n) r} \right)^{\frac{1}{1+n}} \tilde{\sigma}_{ij}(\theta, n, T_z) \tag{4}$$

where J^{far} is so called the far–field J-integral, computed along the contour located at the distance from the crack tip where the plan stress dominates. In Guo's solution the thickness effect entered the final result through functions $T_z(n,r,x_3)$, $I_n(n,T_z)$ and $\tilde{\sigma}_{ij}(n,\theta,T_z)$ where x_3 is the coordinate along the crack front. The computer program and results of computations of $I_n(n,T_z)$ and $\tilde{\sigma}_{ij}(n,\theta,T_z)$ functions were given by Galkiewicz and Graba [2]. The T_z parameter is defined as:

$$T_z = \frac{\sigma_{33}}{\sigma_{11} + \sigma_{22}} \tag{5}$$

The T_z parameter changes from 0 for plane stress to 0.5 for plane strain. It can be considered as an out-of-plane constraint [8].

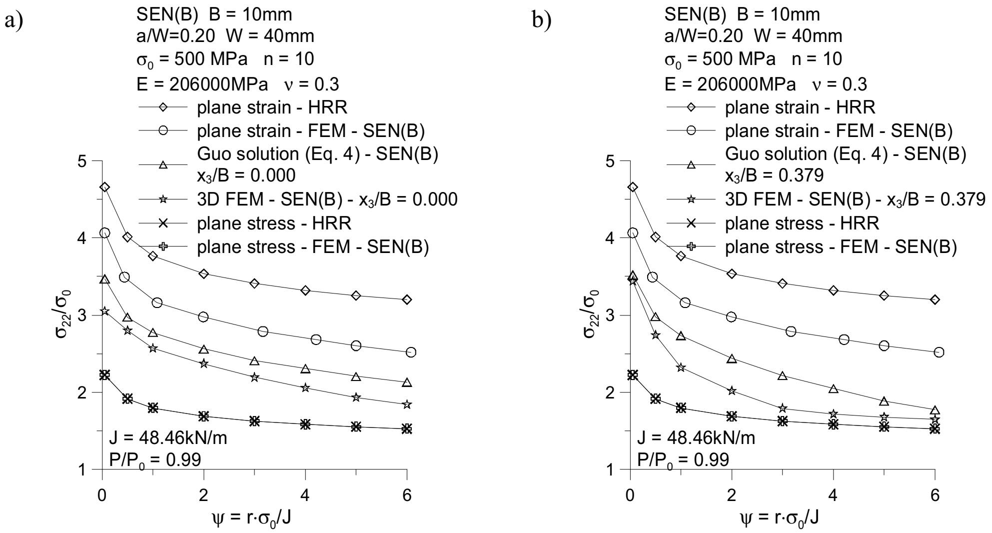

Fig.1. Comparison results for 2D and 3D fracture mechanics for SEN(B) specimen.

In O'Dowd and Shih theory the Q-stress depends on the specimen thickness since it is equal to zero for plane stress and is usually different than zero for plane strain. In Fig. 1. the stress distributions in front of the crack tip, computed using Eq.1, 2 and 4 for plane stress and strain as well as the finite element method (FEM) are compared. It is for one of tested by authors geometries and was selected because of low constraint specimen, the relative crack length is a/W=0.2. In theory the stress and strain fields change with a distance from the crack tip from the plane strain in the middle of the crack front, to the plane stress at the specimen surface or at the distance close to the element thickness. In Fig.2 the changes of a T_z parameter with a distance from the crack front for various distances from the specimen axis are shown. The computations were made for two different R-O exponents and different external loadings.

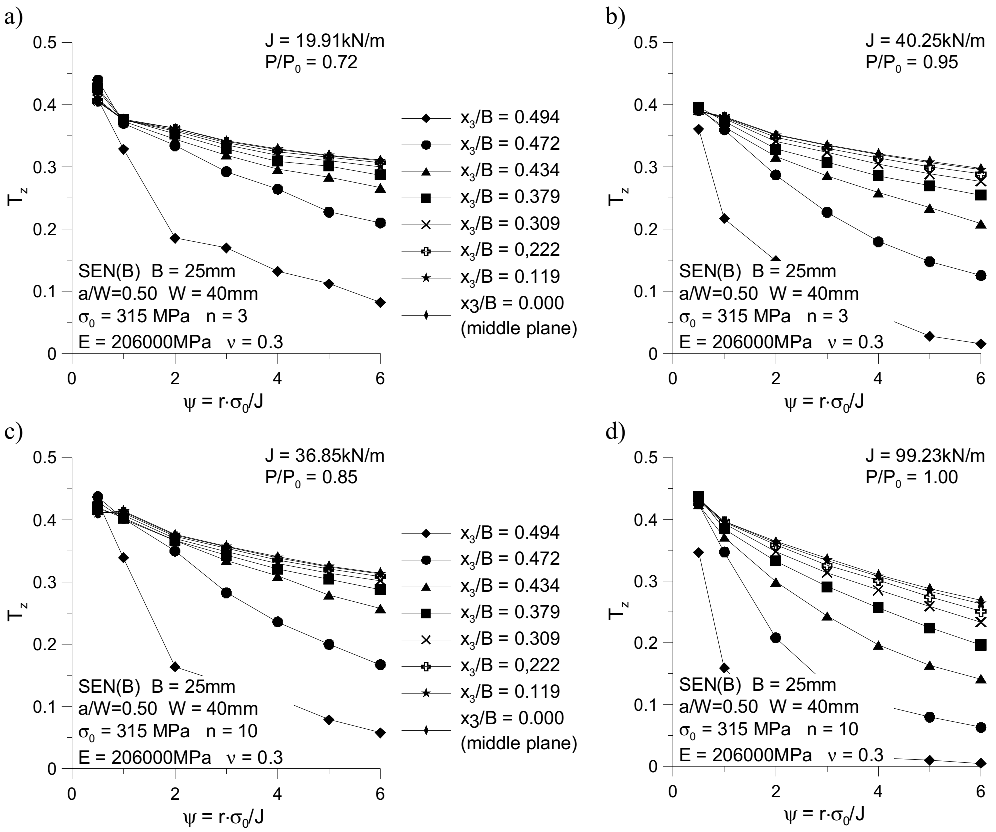

Fig. 2 Radial variation of T_z parameter for different load ratios and two work hardening exponent *n*.

In Fig.3 the changes of the T_z function along the crack front are demonstrated. From the Figs 2 and 3 one can notice that the T_z function does not reach the value of 0.5, characteristic for plane strain, even at the very small distance from the crack front, which is of the order of a crack tip displacement.

1. In – and out-of-plane constraint parameters in one formula

In real elements made of elastic-plastic materials deformation is not small enough in front of the crack to justify an assumption that strains are small. For finite strains the opening stress components reach a maximum value at certain distance from the crack front. This maximum is located at about J/σ_0 distance from the crack front. At the neighborhood of this point the T_z value is usually much smaller then 0.5 (Fig. 3) and the plain strain model may provide conservative results.

We postulate that the stress fields near the crack tip can be described using two terms. Both should take into account the three-dimensional nature of the mechanical fields. The first term is the

Guo term and the second one is a generalization of the Q-parameter. Thus, we propose the following formula:

$$\sigma_{ij} = \sigma_0 \left(\frac{J_{far}}{\alpha \sigma_0 \varepsilon_0 I_n(n,T_z) r} \right)^{\frac{1}{1+n}} \tilde{\sigma}_{ij}(\theta, n, T_z) + Q^*(n, T_z) \sigma_0 \delta_{ij} \tag{6}$$

where $Q^*(n,T_z)$ can be computed from the formula (8)

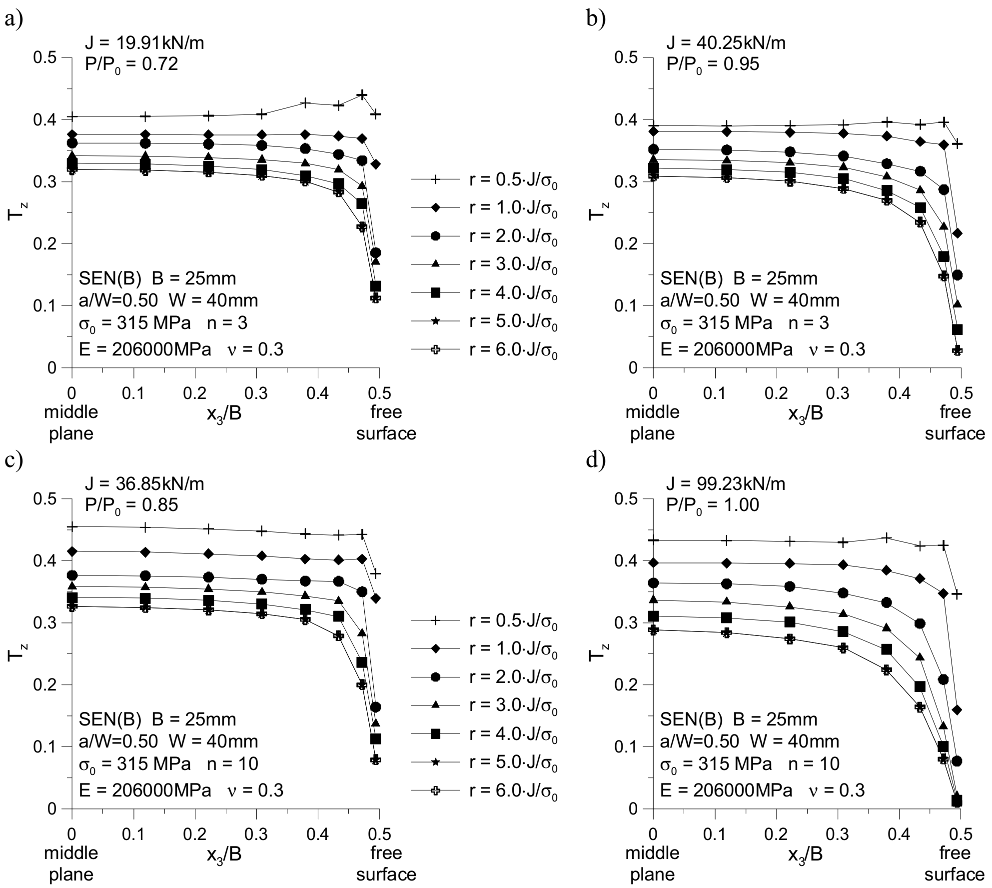

Fig. 3. Variation of T_z parameter through the specimen thickness for different load ratios and R-O exponent n.

Equation 6 allows for computing σ_{ij} values at arbitrary point in front of the 3D crack. An alternative formula, less exact but more convenient to use is proposed in the form

$$\sigma_{ij} = \sigma_0 \left(\frac{J_{far}}{\alpha \sigma_0 \varepsilon_0 I_n(n,T_z \to T_m) r} \right)^{\frac{1}{1+n}} \tilde{\sigma}_{ij}(\theta, n, T_z \to T_m) + Q^*(n, T_z \to T_m) \sigma_0 \delta_{ij} \tag{7}$$

where T_m function is an average through the thickness value of T_z

$$Q^*(n,Tz) = \frac{(\sigma_{\theta\theta})_{FEM} - (\sigma_{\theta\theta})_{GUO}}{\sigma_0} \quad \text{for} \quad \theta=0 \quad \text{and} \quad r = 2\frac{J}{\sigma_0} \tag{8}$$

Since the T_z value strongly depends on a distance from the crack tip (Figs 2 and 3), the Q^* value also depends on these distance. In this paper we compute the Q^* parameter at the distance $2J/\sigma_0$ by analogy to the O'Dowd and Shih approach. Also, we will compute it using the average value of T_z over the distance $(1\div5)J/\sigma_0$ since in this domain the most important failure phenomena take place.

2. Details of numerical model

In the numerical analysis, the single edge notched specimens in bending (SEN(B)) were used Dimensions of the specimens satisfy the ASTM E 1820-05 [9] standard requirements. Computations were performed for three dimensional geometry using small strain option. The relative crack length was a a/W={0.20 ; 0.50 ; 0.70}where a is a crack length and the width of specimens W was equal to 40mm. Computations were performed using ADINA SYSTEM 8.4 [10]. Due to the symmetry, only a quarter of the specimen was modeled. The finite element mesh was filled with the 20-node three dimensional brick elements. The size of the finite elements in the radial direction was decreasing towards the crack tip, while in the angular direction the size of each element was kept constant. The crack tip region was modeled using 36 semicircles. The first of them was 20 times smaller then the last one. It also means, that the first finite element in front of the crack tip is 2000 times smaller then the width of the specimen. The crack tip was modeled as quarter of the arc which radius was equal to $r_w=5\cdot10^{-6}$m ($0.000125\times W$). The mesh consists of eight layers of elements (through half of the thickness of the SEN(B) specimen). The layer interfaces are located at x_3/B={0 ; 0.119 ; 0.222 ; 0.309 ; 0.379 ; 0.434 ; 0.472 ; 0.494 ; 0.5}. It should be noted that the layers become thinner as the free surface is approached. The layer in the middle of the specimen is twenty times thicker then the one near the free surface. The whole SEN(B) specimen was modeled using 2488 finite elements and 12142 nodes.

Table 1. The mechanical properties of the materials used in numerical analysis.

σ_0 [MPa]	E [MPa]	ν	$\varepsilon_0=\sigma_0/E$	α	n	$\tilde{\sigma}_{\theta\theta}(\theta=0)$ for plane strain	I_n for plane strain
315	206000	0.3	0.00153	1	3	1.94	5.51
500			0.00243		5	2.22	5.02
1000			0.00485		10	2.50	4.54
1500			0.00728		20	2.68	4.21

In the FEM simulation, the deformation theory of plasticity and the von Misses yield criterion were adopted. In the model the stress–strain curve was approximated by the relation:

$$\frac{\varepsilon}{\varepsilon_0} = \begin{cases} \sigma/\sigma_0 & \text{for } \sigma \le \sigma_0 \\ \alpha(\sigma/\sigma_0)^n & \text{for } \sigma > \sigma_0 \end{cases} \tag{9}$$

where α=1. The tensile properties of the materials which were used in the numerical analysis are presented in the Table 1. In the FEM analysis, calculations were made for sixteen combinations of the yield stress and the work hardening exponent n. The J–integral was calculated using the "virtual shift method" concept. In the numerical analysis 48 SEN(B) specimens were tested.

3. Numerical results

In Figure 4 the results obtained for several models are compared. Since we assume that the FEM results for 3D model of a specimen are the most accurate, all results are presented as a relative differences with respect to this model.

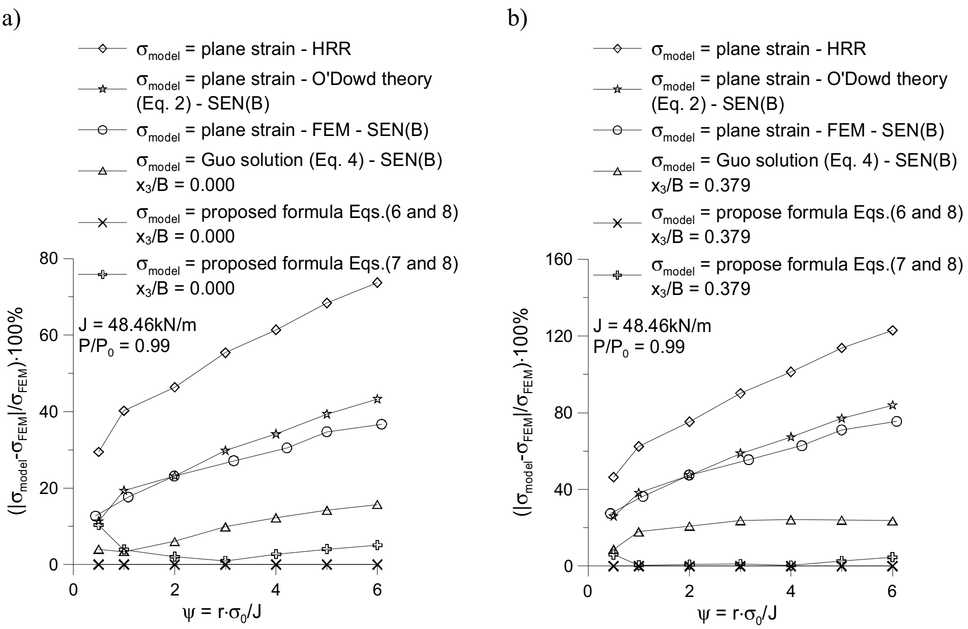

Fig.4. Comparison proposed models of the description the stress field near the crack tip with existing models for SEN(B) specimen: a/W=0.20, B=10mm, W=40mm, σ_0=500MPa, n=10, E=206000MPa, ν=0.30, $\varepsilon_0=\sigma_0/E$=0.00243 (σ_{FEM} for x_3/B=0.000 (a) and x_3/B=0.379 (b)).

Figures 4 and 5-6 are representative of other results received in this research project. More results will be published soon. Guo results are more exact than received using the HRR field. Guo included into analysis the out-of-plane constraint effect. O'Dowd and Shih approximation as well as Yang, Chao and Sutton [11] results are also more exact than received using the HRR formula . They take into account the in-plane constraint influence. Results obtained using our extensions of the Guo, O'Dowd and Shih or Yang, Chao and Sutton models are more exact and they include both the in-plane and out of plane constraint.

4. Summary

The analytical-numerical hybrid method proposed to assess the stress field near the crack tip for elastic-plastic material provides better accuracy than the milestone results by Hutchinson [1], Rice and Rosengren [12] or later excellent papers by Guo[5-7], O'Dowd and Shih [3,4] or Yang, Chao and Sutton [11]. It requires the numerical efforts to compute the Q^* function, which depends on several variables. The T_z function depends on many variables. They are: Ramberg-Osgood power exponent, n, σ_0/E, distance from the crack tip, r, x_3 coordinate, the element thickness and the external loading. However, it is possible and the research is on the way, to receive a simplified semi-analytical formulas both for T_z (it was done for small scale yielding by Guo) and for the Q^*

function with the coefficients computed numerically. Authors of this papers are working on such a catalogue.

Eqs 6 and 7 contain two parameters which allow to include both the in-plane and out-of-plane constraint measures into models to compute an actual value of fracture toughness. Both measures of geometrical constraint are important for ductile materials [8].

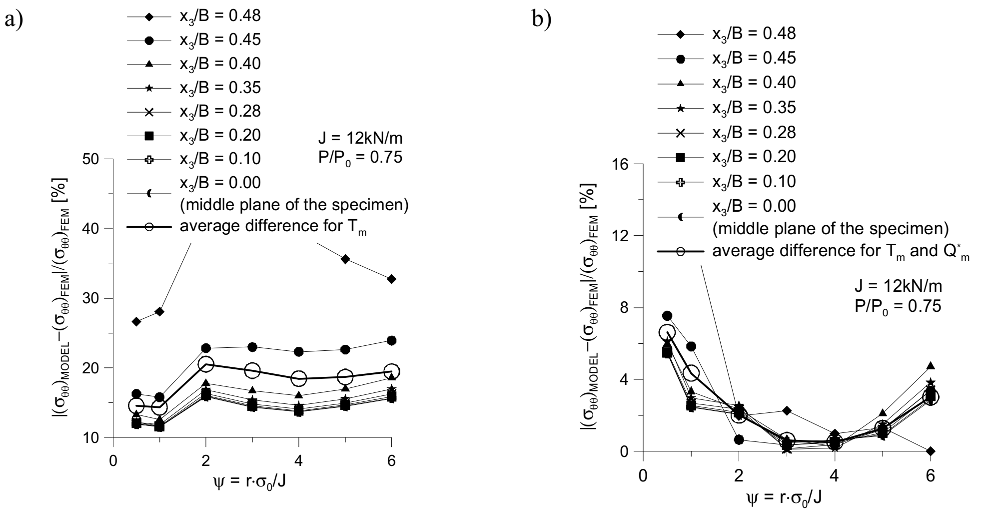

Fig.5. Comparison of the errors with respect to the 3D FEM results a) Guo description (Eq. 4); b) proposed model by Eq. (6,8) for SEN(B) specimen: a/W=0.50, B=25mm, W=40mm, σ_0=315MPa, n=5, E=206000MPa, ν=0.30, $\varepsilon_0=\sigma_0/E$=0.00153 (P/P_0=0.75).

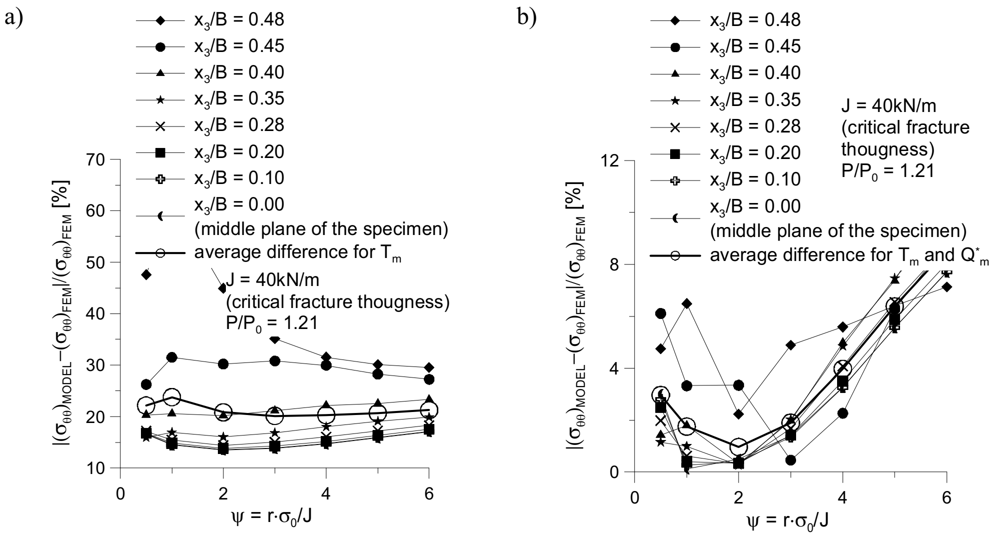

Fig.6. Comparison of the errors with respect to the 3D FEM results a) Guo description (Eq. 4); b) proposed model by Eq. (6,8) for SEN(B) specimen: a/W=0.50, B=25mm, W=40mm, σ_0=315MPa, n=5, E=206000MPa, ν=0.30, $\varepsilon_0=\sigma_0/E$=0.00153 (P/P_0=1.21).

Acknowledgements

The support of the Polish Ministry of Science and Higher Education through the grant **N504 004 31/0106** is acknowledged for the first author and **N501 264334** for the second author.

References

[1] **Hutchinson J.W.** (1968), Singular Behaviour at the End of a Tensile Crack in a Hardening Material, *Journal of the Mechanics and Physics of Solids*, 16, pp.13-31

[2] **Gałkiewicz J., Graba M.,** (2006), Algorithm for Determination of $\tilde{\sigma}_{ij}(n,\theta)$, $\tilde{\varepsilon}_{ij}(n,\theta)$, $\tilde{u}_i(n,\theta)$, $d_n(n)$ and $I_n(n)$ Functions in Hutchinson-Rice-Rosengren Solution and its 3d Generalization, *Journal of Theoretical and Applied Mechanics*, Vol. 44, No. 1, pp. 19-30

[3] **O'Dowd N.P., Shih C.F.** (1991), Family of Crack-Tip Fields Characterized by a Triaxiality Parameter – I. Structure of Fields, *J. Mech. Phys. Solids*, vol. 39, No. 8, pp. 989-1015

[4] **O'Dowd N.P., Shih C.F.** (1992), Family of Crack-Tip Fields Characterized by a Triaxiality Parameter – II. Fracture Applications, *J. Mech. Phys. Solids*, vol. 40, No. 5, pp. 939-963

[5] **Guo Wanlin** (1993), Elastoplastic three dimensional crack border field– I. Singular structure of the field, *Engineering Fracture Mechanics*, Vol. 46, No. 1, pp. 93-104

[6] **Guo Wanlin** (1993), Elastoplastic three dimensional crack border field– II. Asymptotic solution for the field, *Engineering Fracture Mechanics*, Vol. 46, No. 1, pp. 105-113

[7] **Guo Wanlin** (1995), Elasto-plastic three-dimensional crack border field– III. Fracture parameters, *Engineering Fracture Mechanics*, Vol. 51, No. 1, pp. 51-71

[8] **Neimitz A., Gałkiewicz J.** (2006), Fracture toughness of structural components: influence of constraint, *International Journal of Pressure Vessels and Piping*, Vol. 83, pp. 42-54

[9] **ASTM E 820-05**, Standard Test Method for J-integral Characterization of Fracture Toughness.

[10] **ADINA** – Theory and Modeling Guide; Report ARD 04-7; ADINA R& D, Inc.

[11] **Yang S., Chao Y.J., Sutton M.A.** (1993), Higher Order Asymptotic Crack Tip in a Power Law Hadening Material, *Engineering Fracture Mechanics*, Vol. 45, No. 1, 99. 1 – 20

[12] **Rice J.R., Rosengren G.F.** (1968), Plane Strain Deformation Near a Crack Tip in a Power-law Hardening Material, *Journal of the Mechanics and Physics of Solids*, 16, pp.1-12.